HIF2α signaling inhibits adherens junctional disruption in acute lung injury

Haixia Gong,[1,2] Jalees Rehman,[1,2,3] Haiyang Tang,[1,2] Kishore Wary,[1,2] Manish Mittal,[1,2] Pallavi Chatturvedi,[1,2] Youyang Zhao,[1,2] Yulia A. Komorova,[1,2] Stephen M. Vogel,[1,2] and Asrar B. Malik[1,2]

[1]Department of Pharmacology, [2]Center for Lung and Vascular Biology, and [3]Section of Cardiology, Department of Medicine, University of Illinois, College of Medicine, Chicago, Illinois, USA.

Vascular endothelial barrier dysfunction underlies diseases such as acute respiratory distress syndrome (ARDS), characterized by edema and inflammatory cell infiltration. The transcription factor HIF2α is highly expressed in vascular endothelial cells (ECs) and may regulate endothelial barrier function. Here, we analyzed promoter sequences of genes encoding proteins that regulate adherens junction (AJ) integrity and determined that vascular endothelial protein tyrosine phosphatase (VE-PTP) is a HIF2α target. HIF2α-induced VE-PTP expression enhanced dephosphorylation of VE-cadherin, which reduced VE-cadherin endocytosis and thereby augmented AJ integrity and endothelial barrier function. Mice harboring an EC-specific deletion of *Hif2α* exhibited decreased VE-PTP expression and increased VE-cadherin phosphorylation, resulting in defective AJs. Mice lacking HIF2α in ECs had increased lung vascular permeability and water content, both of which were further exacerbated by endotoxin-mediated injury. Treatment of these mice with Fg4497, a prolyl hydroxylase domain 2 (PHD2) inhibitor, activated HIF2α-mediated transcription in a hypoxia-independent manner. HIF2α activation increased VE-PTP expression, decreased VE-cadherin phosphorylation, promoted AJ integrity, and prevented the loss of endothelial barrier function. These findings demonstrate that HIF2α enhances endothelial barrier integrity, in part through VE-PTP expression and the resultant VE-cadherin dephosphorylation-mediated assembly of AJs. Moreover, activation of HIF2α/VE-PTP signaling via PHD2 inhibition has the potential to prevent the formation of leaky vessels and edema in inflammatory diseases such as ARDS.

Introduction

The disruption of the vascular endothelial barrier is a central factor in the protein-rich edema formation and inflammatory cell infiltration that characterize diseases such as acute respiratory distress syndrome (ARDS) (1, 2). Hypoxia-inducible factors (HIFs), composed of oxygen-regulated α subunits and a stable β subunit (3), are essential for mediating adaptive responses to hypoxia and tissue ischemia (4, 5). The mammalian genome encodes 3 HIFα isoforms that can form heterodimers with β subunit and drive gene transcription by recognizing and binding hypoxia response elements (HREs) in gene promoters (6, 7). Hydroxylation of at least 1 critical proline in the oxygen-dependent degradation domain (ODDD) of HIF1α and HIF2α mediates the interaction of HIFs with von Hippel–Lindau E3 ubiquitin ligase complex to ubiquitinate HIFs for proteasomal degradation during ambient normoxia (8, 9). Hydroxylation is catalyzed by 3 known prolyl hydroxylases (PHDs) (8–11). Furthermore, transactivation of HIFs is also regulated by factor-inhibiting HIF1 (FIH1), which blocks binding of HIFα subunits to the transcriptional coactivator factor p300 (12, 13). Hypoxia inhibits the activity of both PHDs and FIH1, leading to nuclear translocation of HIFα subunits and their transcriptional activity (6).

Global *Hif1a* deletion in mice is embryonically lethal due to severely defective vessel formation and neural tube closure (14). However, mice with endothelial-selective deletion of *Hif1a* are viable, and the adult mice demonstrate impaired angiogenesis that has been ascribed to reduced production of paracrine factors such as VEGF (15). Global *Hif2a* deletion also induces embryonic or perinatal lethality, which is associated with bradycardia (16), mitochondrial dysfunction (17), and defective lung and vascular development (18). However, mice developed normally after endothelial deletion of *Hif2a* but displayed aberrant endothelial cell (EC) ultrastructure, coupled with decreased expression of extracellular matrix proteins and increased microvessel leakiness (19). These findings suggest a key role for EC-expressed HIF2α in regulating EC homeostasis in general and the endothelial barrier function in particular.

With regard to regulation of endothelial barrier function, VE-cadherin, a transmembrane glycoprotein forming homophilic *cis* and *trans* dimers essential for the development of inter-EC adherens junctions (AJs), may be targeted by HIF2α (20). VE-cadherin dimer disassembly is in large part regulated by VE-cadherin endocytosis from AJs, activated by phosphorylation of VE-cadherin and its uncoupling from catenin partners, specifically p120-catenin (21, 22). Hence, VE-cadherin endocytosis functions as an important mechanism of AJ disassembly and increased endothelial permeability induced by inflammatory mediators (21, 23). Recent studies have shown that the interaction between VE-cadherin and VE-PTP, an EC-specific transmembrane phosphatase and also a VE-cadherin binding partner, stabilizes VE-cadherin at AJs through dephosphorylation of tyrosine residues on VE-cadherin (24). Because little is known about the role of VE-PTP in regulating the assembly of AJs, in the present study, we addressed the rela-

Authorship note: Haixia Gong and Jalees Rehman contributed equally to this work.
Conflict of interest: The authors have declared that no conflict of interest exists.
Submitted: June 25, 2014; **Accepted:** November 25, 2014.
Reference information: *J Clin Invest*. 2015;125(2):652–664. doi:10.1172/JCI77701.

tionship between VE-PTP and VE-cadherin and its role in regulating the endothelial barrier at the level of AJs. We describe herein the key role of HIF2α signaling in increasing VE-PTP expression and regulating VE-cadherin localization at AJs by restricting VE-cadherin internalization. We also demonstrate that PHD2 inhibition has the potential to strengthen AJs as well as prevent pulmonary edema and neutrophil transmigration induced by endotoxin. Together, our results show that PHD2 inhibition–mediated activation of HIF2α/VE-PTP signaling represents one of the adaptive anti-inflammatory mechanisms that contributes to the restoration of endothelial barrier integrity in inflammatory diseases such as endotoxin-induced acute lung injury.

Results

HIF2α induces expression of VE-PTP and promotes endothelial AJ integrity. We observed that hypoxia exposure stabilized both HIF1α and HIF2α in human lung microvascular ECs (HLMVECs) (Figure 1A). We analyzed the *VEPTP* promoter, because this key AJ protein is upregulated in hypoxia (25), and identified that the *VEPTP* promoter harbored 4 putative HREs (Figure 1B). We performed a ChIP assay to determine the interactions between HIFα subunits and the promoters of *VEPTP* and its binding partner VE-cadherin in ECs. We observed that hypoxia increased HIF2α binding to the *VEPTP* promoter, while this was not the case with HIF1α (Figure 1C). Using a luciferase promoter activity reporter assay, we observed that the presence of HRE2 increased the activity of luciferase by 7 fold, and the activity was increased by 11.5 fold when HRE2 was coexpressed with degradation-resistant HIF2α-mutant HIF2α-DPA (Figure 1D). In contrast, HRE3 and HRE4 failed to further increase luciferase activity (Figure 1D). HRE1 doubled the luciferase activity, a response that might be independent of HIF2α, given that HIF2α-DPA coexpression did not further increase the activity of luciferase (Figure 1D). Thus, HRE2 within the *VEPTP* promoter region was critical for HIF2α-mediated transactivation.

The expression of VE-PTP protein was increased 3 fold by hypoxia, and the response was abrogated following depletion of HIF2α by siRNA or shRNA (Figure 1, E and F). Hypoxia-induced expression of VE-cadherin protein was increased 3 fold, and the response was also HIF2α dependent (Figure 1, E and G). Analysis of mRNA changes showed a 3-fold increase in *VEPTP* mRNA expression (Figure 1H). VE-cadherin mRNA expression, however, was not significantly elevated in hypoxia (Figure 1H), suggesting that hypoxia induction of VE-cadherin protein expression was secondary to a posttranscriptional mechanism. Visualization of VE-cadherin junctions showed that HIF2α depletion also mitigated hypoxia-induced immunostaining of VE-cadherin at AJs (Figure 1I).

Hypoxia-induced enhancement of the endothelial barrier is mediated by HIF2α. We then evaluated whether the hypoxia-induced increases in VE-cadherin and AJs also resulted in functional enhancement of the endothelial barrier and whether this effect was mediated via HIF2α. We observed that transendothelial permeability of the Alexa Fluor 555–conjugated albumin tracer in HLMVEC monolayers was reduced following hypoxia (Figure 2A), consistent with a hypoxia-induced enhancement of the endothelial barrier. This reduction in endothelial permeability was prevented by HIF2α depletion, but not by depletion of HIF1α or HIF3α (Figure 2A). HIF1α and HIF3α depletion also did not prevent hypoxia-induced increases in VE-PTP and VE-cadherin expression levels (Figure 2, B and C). Furthermore, depletion of FIH1, a key regulator of HIF activity, failed to stabilize HIF2α and also did not affect HIF2α-dependent VE-PTP and VE-cadherin upregulation (Figure 2D). Together, these studies suggest that HIF2α is the key mediator of hypoxia-induced enhancement of the endothelial barrier.

HIF2α-induced VE-PTP expression mediates AJ integrity through a reduction of VE-cadherin endocytosis. VE-PTP, through its interaction with VE-cadherin, regulates dephosphorylation of VE-cadherin (24), which is important in regulating VE-cadherin endocytosis–mediated internalization and hence determines the integrity of AJs (21, 22). We therefore determined whether VE-PTP regulated VE-cadherin stability at AJs by modulating VE-cadherin internalization through an endocytotic mechanism. We first demonstrated that hypoxia exposure reduced the phosphorylation of VE-cadherin in an HIF2α-dependent manner (Figure 3, A and B). We also observed that depletion of VE-PTP promoted VE-cadherin phosphorylation at Y658, Y685, and Y731 and thereby suppressed total VE-cadherin expression (Figure 3C). To rescue VE-PTP function in VE-PTP–depleted HLMVECs, we overexpressed a MYC-tagged C-terminal mouse VE-PTP fragment (MYC-VE-PTP-C). This restored both VE-cadherin expression (Figure 3D) and endothelial permeability (Figure 3E). In addition, immunofluorescence studies showed that siRNA-induced depletion of VE-PTP in ECs augmented VE-cadherin internalization via endocytosis (Figure 3, F and G). These studies were conducted by acid washing confluent ECs treated with chloroquine to visualize only internalized vesicle-associated VE-cadherin, which colocalized with endosomal marker EEA1 (refs. 21–23 and Figure 3F). In control cells, hypoxia reduced VE-cadherin internalization when compared with that of normoxia, whereas VE-cadherin internalization was greatly increased following VE-PTP depletion and was further increased when these cells were exposed to hypoxia (Figure 3, F and G). Thus, VE-PTP–mediated inhibition of VE-cadherin internalization was essential for the localization of VE-cadherin at AJs and hence was essential for the assembly of AJs.

EC-specific Hif2a deletion suppresses VE-PTP expression and increases lung vascular permeability. To address whether HIF2α-induced assembly of AJs through the induction of VE-PTP regulated vascular permeability in vivo, we used mice with an inducible EC-restricted *Hif2a* deletion ($Hif2a^{EC-/-}$). In this experiment, expression of VE-PTP, along with VE-cadherin, was significantly decreased in mouse lung microvascular ECs (MLMECs), and this was coupled with increased VE-cadherin phosphorylation at Y658, Y685, and Y731 (Figure 4, A and B), the residues responsible for regulating VE-cadherin–mediated endothelial barrier function (26, 27).

To determine whether the decreased VE-cadherin expression in $Hif2a^{EC-/-}$ mice was secondary to compromised VE-PTP availability, we expressed MYC-VE-PTP-C in $Hif2a^{EC-/-}$ MLMECs. Here, we observed that VE-PTP rescued VE-cadherin expression and partially restored VE-cadherin–dependent endothelial barrier function in the monolayer (Figure 4C). Importantly, lung microvessels of $Hif2a^{EC-/-}$ mice were hyper-permeable to the Evans blue albumin (EBA) tracer, and the lungs were also edematous both during the basal state and in response to LPS challenge compared with those of WT ($Hif2a^{fl/fl}$) mice (Figure 4, D and E). As a further indication of endothelial barrier leakiness, $Hif2a^{EC-/-}$

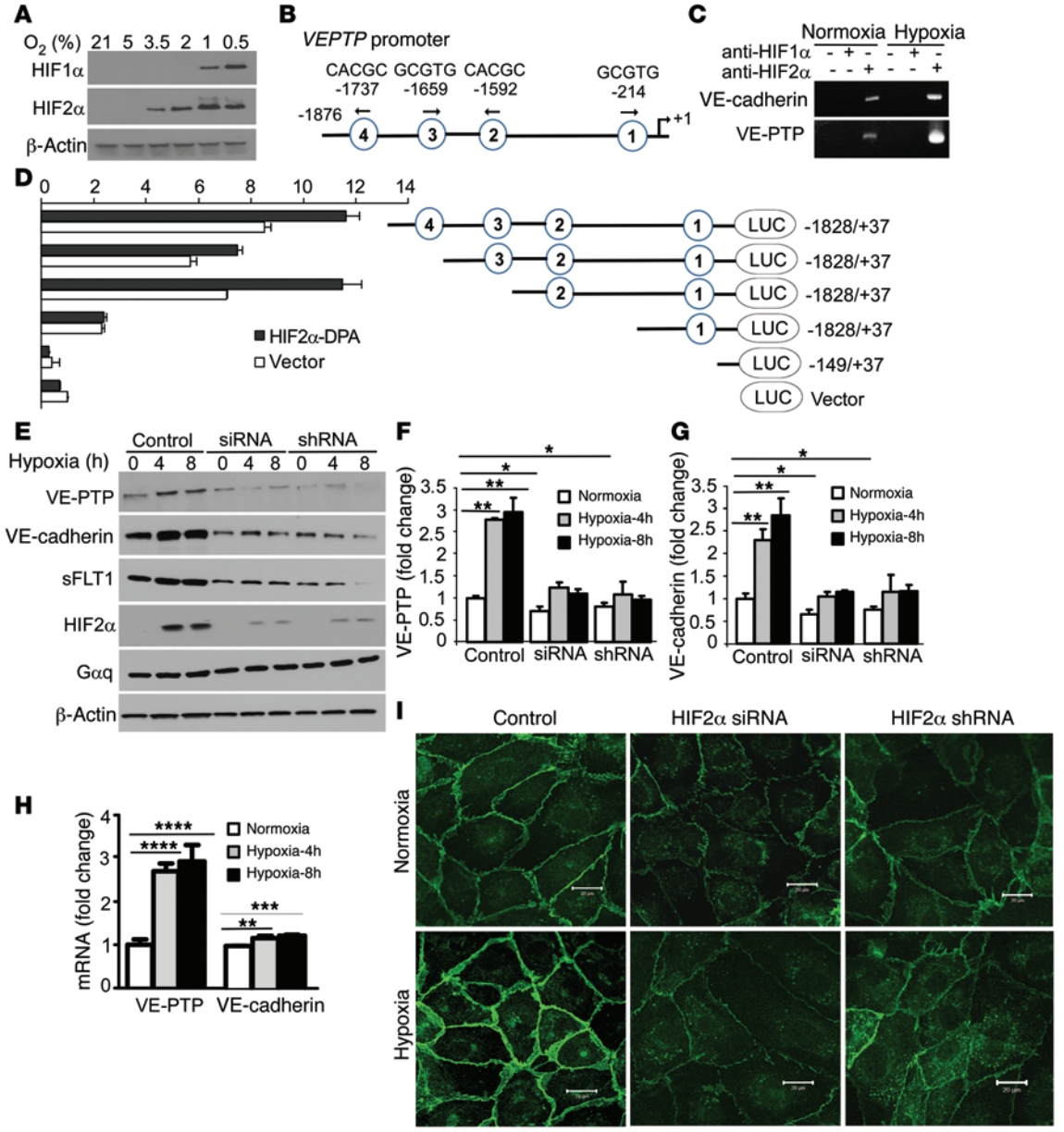

Figure 1. HIF2α induces VE-PTP expression and enhances the integrity of endothelial AJs. (**A**) HLMVECs were exposed to varying concentrations of O_2 for 8 hours. Expression of HIF1α and HIF2α was assessed by WB. (**B**) Representation of the *VEPTP* promoter region. HREs are shown by circled numbers, and their sequences are displayed. (**C**) HLMVECs were exposed to normoxia or 1% O_2 for 8 hours. A ChIP assay was performed to amplify the *VEPTP* and VE-cadherin promoters. (**D**) 293T cells were transfected with an HIF2α-DPA expression plasmid containing luciferase reporter constructs. Luciferase values were normalized to β-gal values. A schematic representation of corresponding deletion constructs is presented in the right panel. (**E**) HLMVECs infected with lentiviral HIF2α siRNA/shRNA were exposed to normoxia or 1% O_2. Expression of VE-cadherin, VE-PTP, and HIF2α was assessed by WB. (**F**–**G**) Quantification of VE-PTP (**F**) and VE-cadherin (**G**) protein levels. (**H**) HLMVECs were exposed to normoxia or 1% O_2. Expression of *VEPTP* and VE-cadherin at the mRNA level was assessed by quantitative PCR. (**I**) AJ integrity of HLMVECs was examined by VE-cadherin immunostaining using confocal microscopy. Scale bars: 20 μm. n = 3/group (**F**–**H**). Blot images were derived from samples run on parallel gels. *$P < 0.05$; **$P < 0.01$; ***$P < 0.005$; ****$P < 0.001$ by Student's t test.

mice exhibited an increased lung microvessel filtration coefficient ($K_{f,c}$), an index of vascular permeability to fluid when compared with that of control *Hif2a*$^{fl/fl}$ mice (Figure 4F). We also observed increased leukocyte infiltration, as evidenced by increased leukocyte counts in bronchoalveolar lavage (BAL) fluid from the lungs of *Hif2a*$^{EC-/-}$ mice compared with that detected in controls (Figure 4G). The mortality rate of *Hif2a*$^{EC-/-}$ mice was greater than that of *Hif2a*$^{fl/fl}$ mice after a sublethal dose of LPS (Figure 4H) as well as after a cecal ligation and puncture (CLP) model of sepsis (Figure 4I), consistent with severe lung congestion and infiltration of inflammatory cells in this model.

PHD2 regulates endothelial barrier function through HIF2α-dependent expression of VE-PTP and VE-cadherin. We next addressed whether inhibition of PHD2 hydroxylation, the upstream

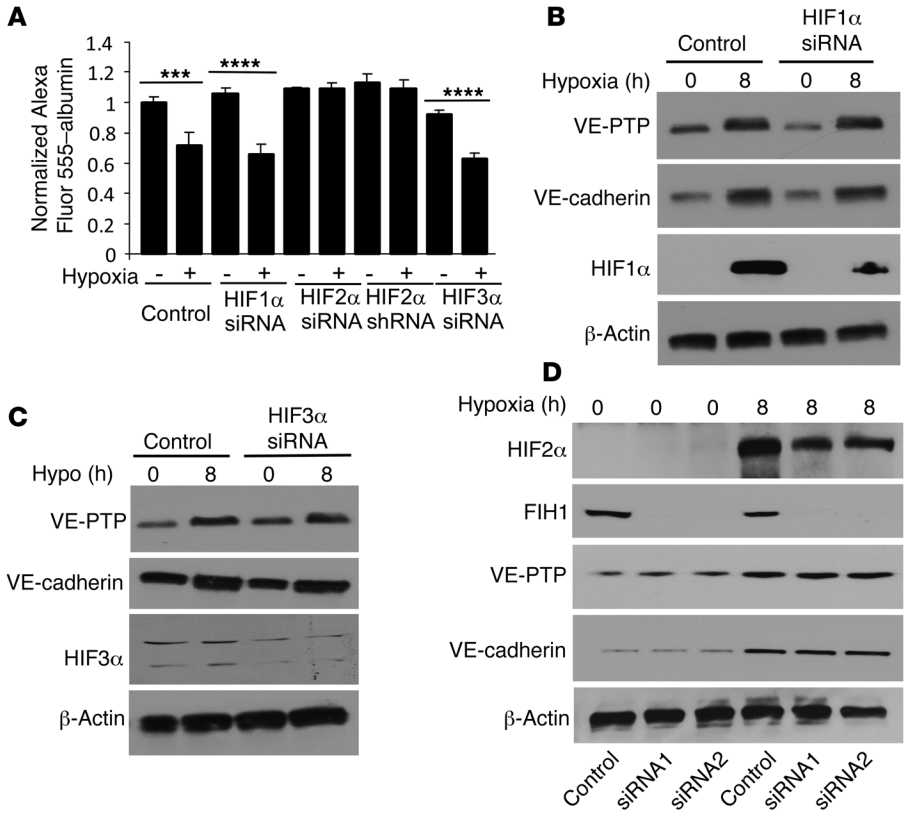

Figure 2. Hypoxia-induced stabilization of the endothelial barrier is mediated by HIF2α. (**A**) Control, HIF1α-, HIF2α-, or HIF3α-depleted HLMVECs were grown on Transwell plates and exposed to 1% O_2 (hypoxia) for 8 hours with an Alexa Fluor 555–albumin tracer to assess endothelial barrier permeability. Tracer concentrations were determined in the lower-chamber media. ***$P < 0.005$, ****$P < 0.001$ by Student's *t* test. (**B**–**D**) HLMVECs infected with lentiviral control vector, HIF1α siRNA (**B**), HIF3α siRNA (**C**), or FIH1 siRNA (**D**) were exposed to normoxia or 1% O_2. Expression of the indicated proteins was evaluated by WB. *n* = 3/group (**A**–**D**). Blot images were derived from samples run on parallel gels.

step in HIF activation, was involved in strengthening the endothelial barrier through stabilization of HIF2α and the subsequent increased expression of VE-PTP. In these studies, HIF2α stabilization achieved by depletion of PHD2 resulted in increased VE-PTP expression and reduced VE-cadherin phosphorylation at Y658, Y685, and Y731 (Figure 5A). Depletion of PHD2 increased VE-PTP expression by 3 fold (Figure 5B) and VE-cadherin expression by 2.5 fold (Figure 5C). However, neither depletion of PHD1 nor PHD3 had a significant effect (Figure 5D). VE-cadherin immunostaining showed significantly increased intensity of staining following PHD2 depletion (Figure 5, E and F). Moreover, the endothelial barrier was resistant to LPS-induced AJ disassembly (Figure 5G).

To establish the role of PHD2 hydroxylation in mediating VE-PTP expression, we next transfected HLMVECs with the HIF2α-mutant Flag-HIF2α-DPA, which is resistant to hydroxylation and degradation by PHDs (28). Expression of HIF2α-DPA increased the expression of VE-PTP as well as VE-cadherin by preventing VE-cadherin phosphorylation (Figure 6, A–C). Immunostaining showed that expression of the HIF2α-DPA mutant increased AJ formation, whereas the HIF1α-DPA mutant (HA-HIF1α-DPA) had no effect (Figure 6, D and E). These studies support the concept that inhibiting PHD2 function in ECs induces assembly of AJs through HIF2α-mediated upregulation of VE-PTP.

Therapeutic PHD2 inhibition prevents lung vascular leakiness and edema and reduces mortality in a sepsis-induced lung injury model. Since PHD2 depletion in ECs promoted the expression of VE-PTP, stabilized VE-cadherin at AJs, and prevented AJ disassembly in response to LPS, we next determined whether therapeutically inhibiting PHD2 function with the PHD2-specific inhibitor Fg4497 (29) would be beneficial in acute lung injury models. First, we conducted studies by treating HLMVEC monolayers with Fg4497. This increased expression of HIF2α resulted in decreased VE-cadherin phosphorylation at Y658, Y685, and Y731 (Figure 7A). Immunostaining demonstrated increased AJ assembly (Figure 7B). Importantly, Fg4497 also prevented LPS-induced AJ disruption (Figure 7C). This endothelial barrier protection was coupled with increased VE-PTP expression and concomitant VE-cadherin dephosphorylation (Figure 7, D and E). Moreover, Fg4497 also suppressed VE-cadherin internalization from AJs (Figure 7F).

To address whether endothelial AJs could be similarly strengthened in vivo, we treated C57/BL6 mice with an i.v. injection of Fg4497. The increases in expression of VE-PTP and VE-cadherin after treatment lasted up to 5 days (Figure 8A). To test the therapeutic effectiveness, we measured lung endothelial permeability in mice challenged with LPS. Mice pretreated with Fg4497 showed a reduced pulmonary transvascular flux of EBA and wet-to-dry lung weight ratios after LPS challenge (Figure 8, B and C). We also observed that basal transvascular fluid filtration rates in Fg4497-treated mice were markedly reduced compared with those in control lungs (Figure 8D), indicating a strengthening of the endothelial barrier in vivo. Additionally, pretreatment with Fg4497 prevented LPS-induced leukocyte infiltration into the lungs (Figure 8E). We next tested the therapeutic efficacy of PHD2 inhibition after the initiation of LPS- or CLP-induced lung injury. In these studies, mice treated with Fg4497 two hours after LPS challenge had a survival rate of 80% by day 5, whereas the control group had 0% survival at this point (Figure 8F). In the CLP polymicrobial sepsis model, we found a similar survival advantage after Fg4497 treatment (Figure 8G).

Discussion

Here, we have identified the role of the transcription factor HIF2α in strengthening the vascular endothelial barrier through expres-

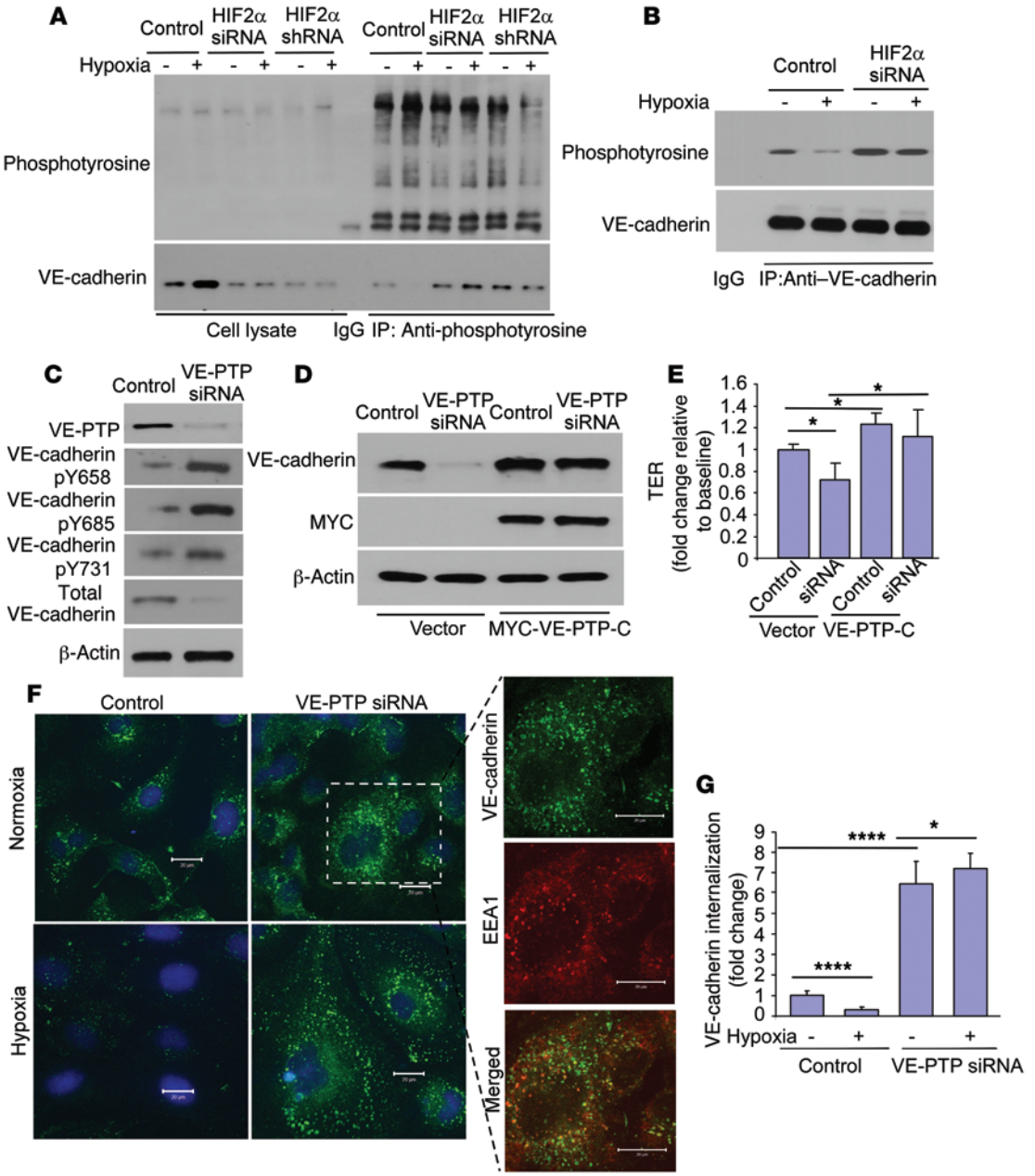

Figure 3. HIF2α-induced VE-PTP expression mediates AJ integrity through retention of VE-cadherin at AJs. (**A** and **B**) HLMVECs were exposed to normoxia or 1% O_2 for 8 hours and harvested in modified RIPA buffer. Cell lysates were precipitated with anti-phosphotyrosine antibody (**A**) or anti–VE-cadherin antibody (**B**), and IPs were then probed by WB using the converse antibody. (**C**) HLMVECs were infected with control or VE-PTP siRNA lentivirus. Expression of VE-VTP and VE-cadherin and phosphorylation of the indicated tyrosines in VE-cadherin were assessed by WB. (**D**) Control and VE-PTP siRNA lentivirus-infected HLMVECs were subjected to overexpression of an active MYC-VE-PTP-C fragment. Expression of VE-cadherin and MYC-VE-PTP-C was detected by WB. (**E**) Permeability of the endothelial monolayer of these cells used in **D** was measured by TER assay under basal conditions (n = 3–4). (**F**) Control and VE-PTP siRNA lentivirus–infected HLMVECs were exposed to normoxia or 1% O_2 for 8 hours, labeled with anti–VE-cadherin antibody (BV9) in the presence of 100 μM chloroquine for 4 hours at 37°C to visualize internalized VE-cadherin in vesicles, and then subjected to a mild acid buffer wash to remove noninternalized VE-cadherin. Cells were fixed and subjected to immunostaining using anti-EEA1 antibody to visualize endosomes. Internalization of VE-cadherin was examined by confocal microscopy. Scale bars: 20 μm. (**G**) Quantification of internalized VE-cadherin puncta from 4 to 8 randomly chosen fields. Blot images were derived from samples run on parallel gels. $^*P < 0.05$, $^{****}P < 0.001$ by Student's t test.

sion of the VE-cadherin–associated tyrosine phosphatase VE-PTP. We demonstrated that HIF2α-induced VE-PTP expression prevented the dephosphorylation of VE-cadherin tyrosine residues Y658, Y685, and Y731 and thereby abrogated the phosphorylation-dependent VE-cadherin internalization via endocytosis from AJs. These results are consistent with our other findings that VE-PTP expression restored VE-cadherin expression and endothelial barrier function in VE-PTP–depleted human ECs and also partially restored endothelial barrier integrity in *Hif2a*$^{EC-/-}$ ECs. Together, the findings suggest that VE-PTP–mediated dephosphorylation

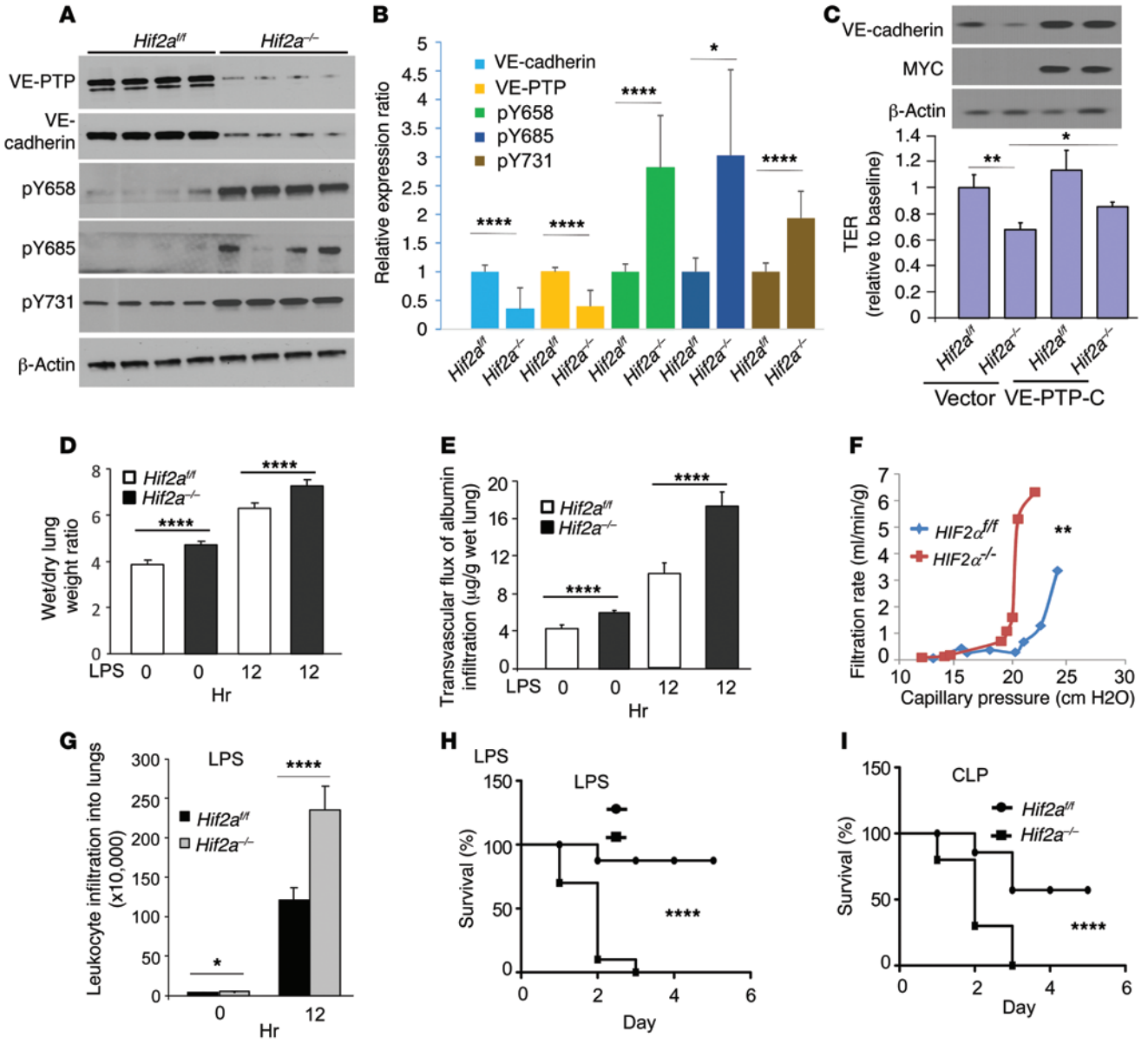

Figure 4. Endothelial-specific *Hif2a* deletion in mice increases lung vascular permeability through suppression of VE-PTP expression and VE-cadherin phosphorylation. (**A**) Dissected lungs of *Hif2a*$^{fl/fl}$ and *Hif2a*$^{EC-/-}$ mice were homogenized in RIPA buffer, and WB was performed to determine expression of the indicated proteins. (**B**) Quantification of VE-PTP and VE-cadherin expression and VE-cadherin phosphorylation (n = 4). (**C**) PMECs isolated from *Hif2a*$^{fl/fl}$ and *Hif2a*$^{EC-/-}$ mice were transduced with control or MYC-VE-PTP-C lentivirus. Expression of MYC-VE-VTP-C and VE-cadherin was assessed by WB. Permeability of the endothelial monolayer was measured by TER assay under baseline normoxic conditions. n = 3–4. (**D**) *Hif2a*$^{fl/fl}$ and *Hif2a*$^{EC-/-}$ mice were challenged with PBS or 15 mg/kg LPS i.p. Wet and dry lung weights were recorded to determine edema. n = 5 /group. (**E**) *Hif2a*$^{fl/fl}$ and *Hif2a*$^{EC-/-}$ mice were injected with PBS or 15 mg/kg LPS. Pulmonary transvascular permeability to EBA was measured by detecting OD620 and OD740 of the formamide extract. Data represent the mean ± SD. n = 5/group. (**F**) Lungs of *Hif2a*$^{fl/fl}$ and *Hif2a*$^{EC-/-}$ mice were isolated, and pulmonary transvascular filtration was assessed. Each plotted point represents a measurement from a different lung preparation. (**G**) Quantification of leukocytes in the BAL fluid from *Hif2a*$^{fl/fl}$ and *Hif2a*$^{EC-/-}$ mice challenged with 15 mg/kg LPS. n = 4/group. (**B**–**G**) $^*P < 0.05$, $^{**}P < 0.01$, $^{****}P < 0.001$ by Student's t test. (**H** and **I**) *Hif2a*$^{fl/fl}$ and *Hif2a*$^{EC-/-}$ mice were challenged with 25 mg/kg LPS i.p. (**H**) or polymicrobial sepsis was induced by CLP (**I**), and survival was monitored. n = 10/group. Differences in mortality were analyzed by log-rank test. Blot images were derived from samples run on parallel gels. $^{****}P < 0.001$ by log-rank test.

of VE-cadherin is a constitutive mechanism that prevents VE-cadherin endocytosis under normoxic conditions in ECs and that hypoxia markedly enhances the endothelial barrier–stabilizing activity of VE-PTP. The fact that VE-PTP overexpression did not completely restore endothelial barrier function in *Hif2a*$^{EC-/-}$ ECs suggests that additional HIF2α targets, such as angiopoietin 2 and DLL4 (19), may also be contributing to the endothelial barrier–stabilizing effects of HIF2α. Importantly, HIF2α activation by hypoxia or PHD2 inhibition prevented the disassembly of AJs and resultant loss of endothelial barrier function in ECs activated by endotoxin.

We set out in these studies to determine the role of HIFs in regulating VE-PTP expression on the basis of the finding that

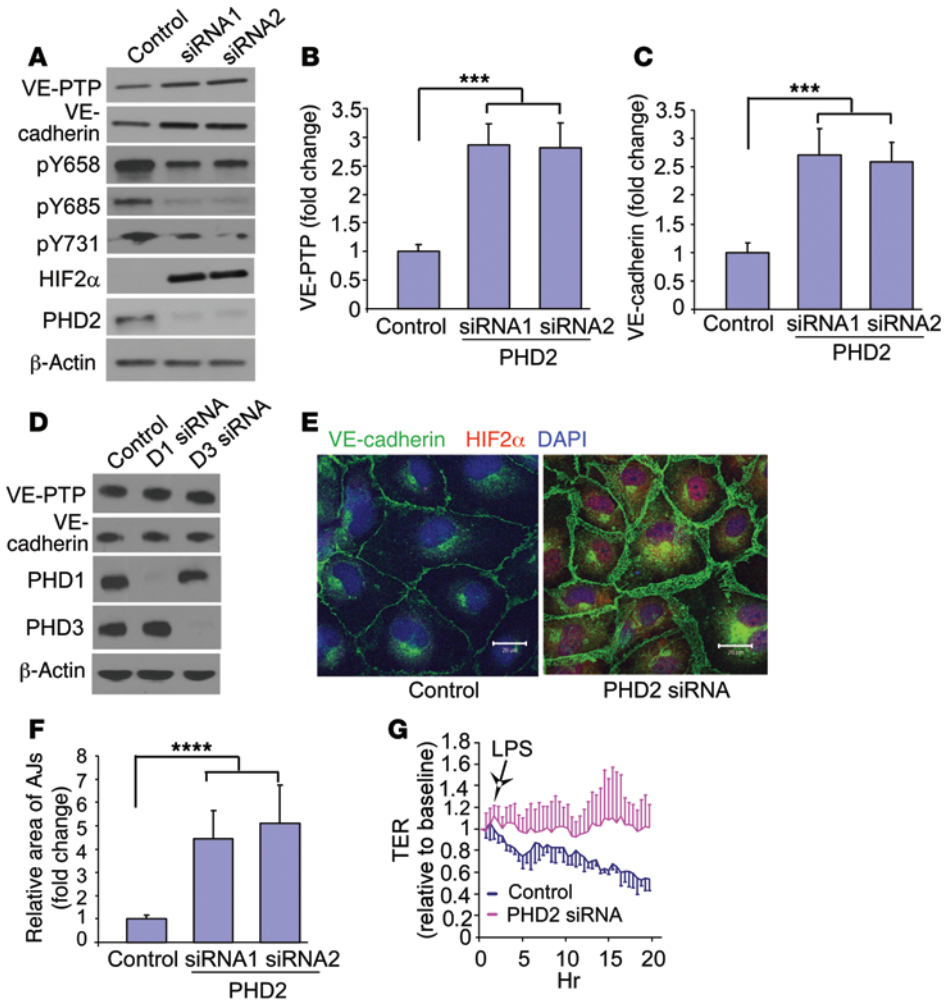

Figure 5. PHD2 depletion enhances the integrity of the endothelial barrier and increases VE-PTP expression. (**A**) HLMVECs were infected with control or lentiviral PHD2 siRNA, and WB was performed to determine the expression of VE-cadherin, VE-PTP, PHD2, and HIF2α as well as the extent of VE-cadherin tyrosine phosphorylation at Y658, Y685, and Y731. (**B** and **C**) Quantification of VE-PTP (**B**) and VE-cadherin (**C**) protein expression following PHD2 depletion (n = 3). (**D**) HLMVECs were infected with control or lentiviral PHD1 and PHD3 siRNAs, and WBs were used to compare expression levels of VE-cadherin, VE-PTP, PHD, and PHD3. (**E**) HLMVECs infected with control or lentiviral PHD2 siRNA were immunostained and analyzed by confocal microscopy. (**F**) Quantification of AJ thickness in random fields (n = 25–35 cells). (**G**) Serum-starved confluent HLMVECs infected with control or lentiviral PHD2 siRNA were challenged with 1 μg/ml LPS, and TER was monitored to determine AJ disassembly. TER values of each monolayer were normalized to baseline values (n = 4/group). ***P < 0.005, ****P < 0.001 by Student's t test.

hypoxia upregulated VE-PTP expression (25, 30). We found that the *VEPTP* promoter harbored 4 HREs, of which HRE2 showed the greatest HIF2α-dependent transctivation and was critical for *VEPTP* mRNA transcription. VE-PTP, an EC-specific transmembrane protein, forms a complex with VE-cadherin at AJs and is believed to mediate the assembly of AJs by VE-cadherin dephosphorylation (24). SRC kinase–dependent VE-cadherin phosphorylation (21) and VE-PTP–mediated dephosphorylation of VE-cadherin are important countervailing regulators of the remodeling and plasticity of AJs (31). We observed that depletion of VE-PTP increased endothelial permeability, consistent with the role of VE-cadherin phosphorylation in the absence of VE-PTP in mediating VE-cadherin internalization via endocytosis and AJ disassembly.

Intriguingly, hypoxia through the activation of HIF2α upregulated VE-PTP and thereby augmented dephosphorylation of VE-cadherin at the 3 tyrosine residues. Dephosphorylation at these sites, in turn, reduced endocytosis-mediated VE-cadherin internalization from AJs and promoted vascular barrier function. Together, these findings suggest a model (Figure 6) in which dephosphorylation of VE-cadherin by VE-PTP is an essential determinant of AJ assembly. In this context, increased VE-PTP expression mediated by HIF2α promotes VE-cadherin interactions at AJs and thus strengthens the endothelial barrier.

We observed that HIF2α-mediated VE-PTP expression was physiologically relevant and represented a fundamental adaptive response to tissue hypoxia and inflammation, both of which are characterized by stabilization and nuclear translocation of HIF2α (32). The importance of this mechanism was evident by the finding that EC-specific deletion of *Hif2a* (*Hif2a*$^{EC-/-}$) in mice enhanced endothelial permeability as well as leukocyte extravasation in lungs secondary to inhibition of VE-PTP expression. Overexpression of MYC-tagged C-terminal VE-PTP enhanced VE-cadherin protein expression and partially restored endothelial barrier function in both VE-PTP–depleted HLMVECs and *Hif2a*$^{EC-/-}$ mouse PMECs, substantiating our findings that VE-PTP is an HIF2α target and one of the upstream regulators of VE-cadherin.

Studies by Vestweber have shown that phosphorylation of the VE-cadherin tyrosine residues Y658 and Y685 regulated endothelial permeability, whereas phosphorylation of Y731 mediated leukocyte extravasation across AJs (21, 26, 33). Since we identified that these 3 residues were dephosphorylated by HIF2α-induced VE-PTP expression, we addressed the possibility that HIF2α is protective in models of sepsis on the basis of the dephosphorylation switch mechanism described above. We observed that EC-specific deletion of *Hif2a* in mice induced lung vascular barrier leakiness and inflammation and also increased the mortality rates in both LPS- and CLP-challenged mice. Thus, HIF2α-dependent upregulation of VE-PTP expression resulting in dephosphorylation of VE-cadherin at Y658, Y685, and Y731 is consistent with the model (Figure 9) that the dephosphorylation switch is a key endogenous barrier–enhancing anti-inflammatory mechanism.

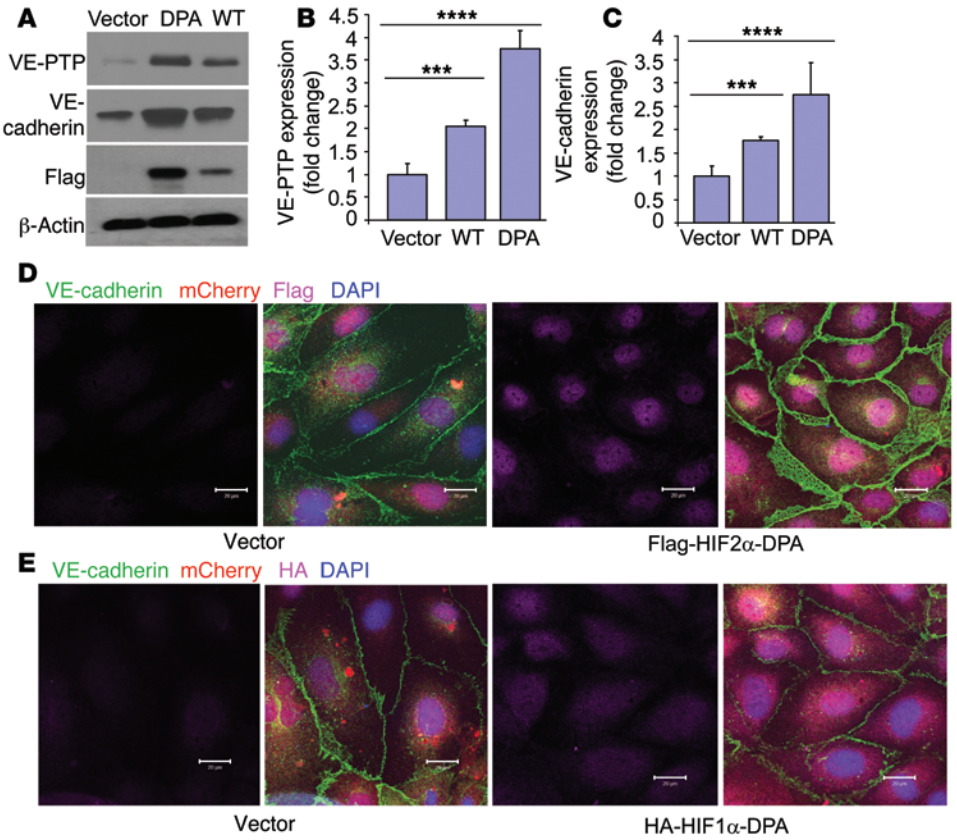

Figure 6. Expression of hydroxylation- and degradation-resistant HIF2α-mutant HIF2α-DPA in HLMVECs stabilizes the endothelial barrier via VE-PTP expression. (**A**) HLMVECs were infected with lentivirus expressing a Flag-tagged WT HIF2α or with a hydroxylation- and degradation-resistant HIF2α-DPA mutant. VE-PTP and VE-cadherin protein expression was determined by WB. Quantification of VE-PTP (**B**) and VE-cadherin (**C**) expression (n = 3/group). (**D** and **E**) HLMVECs infected with lentivirus expressing WT, a HA-HIF1α-DPA mutant, or a Flag-HIF2α-DPA mutant were immunostained for VE-cadherin and analyzed by confocal microscopy. Scale bars: 20 μm. Blot images were derived from samples run on parallel gels. ***P < 0.005, ****P < 0.001 by Student's t test.

We also determined whether hypoxia-independent HIF2α activation through direct inhibition of PHDs could induce expression of VE-PTP and thereby stabilize AJs. Results from siRNA-mediated knockdown of PHD1, PHD2, or PHD3 showed that PHD2 depletion was specific in mediating HIF2α-dependent VE-PTP expression and dephosphorylation of VE-cadherin. To address whether VE-PTP upregulation could be therapeutically targeted, we treated mice with the PHD2 inhibitor Fg4497 (29). In these studies, HIF2α-induced VE-PTP expression markedly reduced inflammatory lung injury and mortality following sepsis. This finding is consistent with a report showing that *Hif2a* deletion enhanced ischemic kidney injury (34), pointing toward a similar protective effect of HIF2α in the setting of kidney injury. Although that study did not specifically examine the role of VE-PTP and vascular barrier integrity, our results suggest that HIF2α-mediated VE-PTP expression in renal vascular ECs likely contributed to the renoprotective effect of HIF2α.

Our studies demonstrate a novel role for the HIF2α/VE-PTP/VE-cadherin cascade in strengthening the endothelial barrier, but we cannot exclude other targets of VE-PTP that may contribute to strengthening of the vascular barrier. VE-PTP not only dephosphorylates VE-cadherin, as we showed, but also couples with and dephosphorylates TIE2, a receptor for both angiopoietin 1 (ANG1) and ANG2, which regulate endothelial permeability and angiogenesis by antagonizing each other (25, 30, 35, 36). In tumors, VE-PTP inhibition normalized the structure and function of tumor vessels through TIE2 activation (35). Since ANG2 contributed to the loss of endothelial barrier function in sepsis (37), it is possible that some of the barrier-enhancing effects observed in our VE-PTP depletion studies may be due to activation of ANG2/TIE2 signaling. It has also been reported that VE-PTP regulates the activity of the endothelial VEGF receptor VEGFR2 via the TIE2 receptor (38), which in turn could affect endothelial barrier function, since VEGF signaling increased vascular permeability (23). Further, since the dissociation of VE-PTP and VE-cadherin is redox dependent (39) and HIF2α favors a reduced redox state (40), HIF2α activation in the endothelium may contribute to enhanced barrier function through suppression of ROS signaling. This reduced redox state may be a reflection of metabolic shifts induced by hypoxia or HIF2α signaling such as enhanced glycolytic activity, which we did not study but which may have contributed to the endothelial barrier–enhancing effects of hypoxia and HIF2α activation.

Our studies shed light on the controversy surrounding the effects of hypoxia on endothelial barrier function. Some studies have observed that hypoxia disrupted the endothelial barrier (41) and that VEGF, which is released in hypoxia, disassembled endothelial AJs by increasing VE-cadherin internalization (23). In contrast, rigorous in vivo studies in the sheep lung lymph fistula model performed by Bland and colleagues showed unequivocally that long-term hypoxia did not increase lung vascular permeability (42, 43). Our results help reconcile these apparently discordant findings. We propose that HIF2α activation serves as an endogenous mechanism to stabilize AJs. During injury and hypoxia, both barrier-disrupting pathways such as VEGF-induced VE-cadherin internalization (23) as well as barrier-restoring pathways such as HIF2α/VE-PTP–induced VE-cadherin stabilization observed by us may be concomitantly activated. Thus, the relative contributions of each of these pathways may ultimately determine endothelial barrier function. The balance between the two is probably contextual, depending on the vascular bed as well as the timing and magnitude of activation of these counterbalancing pathways.

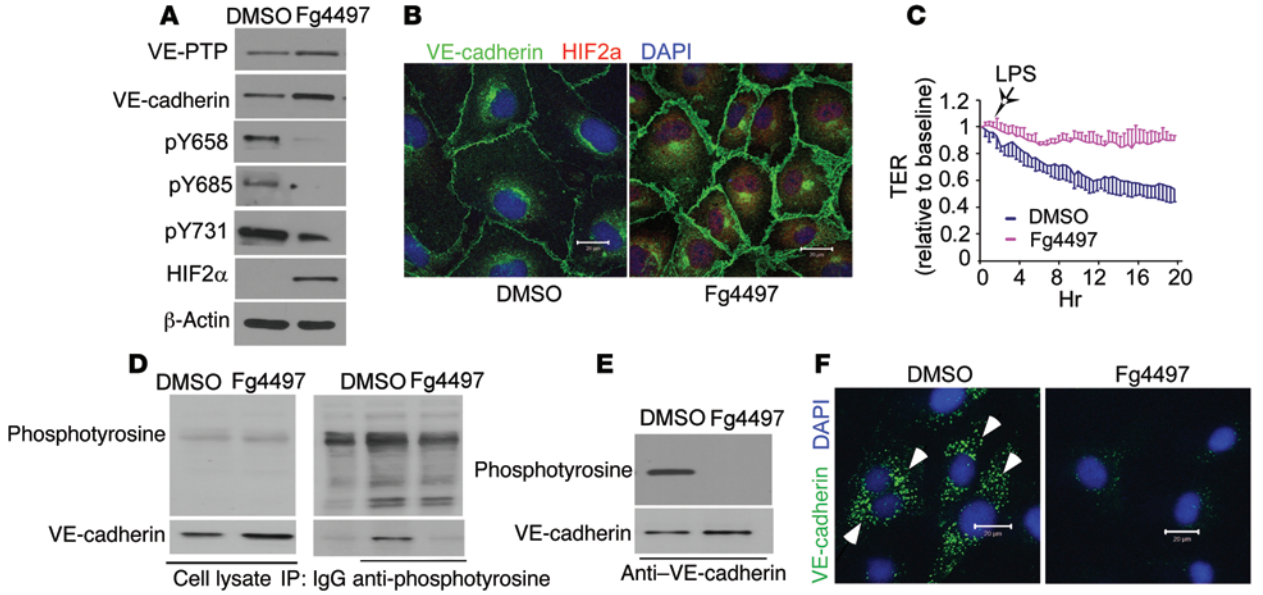

Figure 7. PHD2 inhibition promotes endothelial barrier integrity in vitro. (**A** and **B**) HLMVECs were treated with 10 μM Fg4497 or DMSO for 8 hours. WB (**A**) or immunostaining (**B**) was performed to determine expression levels of the specified proteins. (**C**) HLMVECs pretreated with DMSO or Fg4497 were challenged with 1 μg/ml LPS, and AJ integrity was monitored by TER (n = 3/group). (**D** and **E**) Lysates of HLMVECs pretreated with DMSO or Fg4497 were precipitated with anti-phosphotyrosine (**D**) or anti–VE-cadherin (**E**) antibodies and detected by WB. (**F**) DMSO- or Fg4497-pretreated HLMVECs were labeled with anti–VE-cadherin antibody in the presence of 100 μM chloroquine. Internalization of VE-cadherin (arrowheads) was examined by confocal microscopy. Scale bars: 20 μm. Blot images were derived from samples run on parallel gels.

This concept could reconcile the observation that hypoxia did not cause barrier disruption in the pulmonary vasculature (42) but disrupted aortic EC junctions (41).

The contextual aspect of VE-PTP's role in stabilizing the endothelial barrier also needs to be considered in light of a recent study, which showed that inhibiting VE-PTP by a small-molecule inhibitor stabilized the ocular vasculature in experimental models of retinal neovascularization (30). In that study, the barrier-stabilizing effects of VE-PTP inhibition were attributed to suppression of VEGF-induced permeability as well as increased TIE2 activation, because TIE2 is a binding partner of VE-PTP (32). Our observation that VE-PTP activation stabilizes the endothelial barrier may be explained by differences in TIE2 and VEGF signaling in the ocular vasculature undergoing angiogenesis and by the lung endothelium responding to acute endotoxin-mediated injury.

Hypoxemia secondary to pulmonary edema is a hallmark of ARDS in patients (44). The degree of hypoxemia is a predictor of mortality in these patients, and even though recent attempts to improve oxygenation such as with high-frequency reduced-volume ventilation have reduced hypoxemia, overall mortality rates remain high (45). Since our findings suggest that hypoxia activates an endogenous HIF2α-dependent barrier-protective pathway in the pulmonary endothelium, it may be of value to harness this endogenous endothelial barrier–protective mechanism in ARDS patients.

An intriguing finding was that the observed HIF2α/VE-PTP–mediated stabilization of AJs did not require the presence of hypoxia. The mechanisms by which HIF2α is activated in ECs by endotoxin in the absence of hypoxia are not well understood, but it is known that HIFs are stabilized in response to endotoxin in macrophages (46) and that mitochondrial ROS generation in ECs contributes to HIF activation (47, 48). This is especially important for the translational relevance of these findings, because they suggest that HIF2α is a potential therapeutic target in sepsis before the onset of severe pulmonary edema and hypoxemia. We observed that the small-molecule PHD2 inhibitor Fg4497, which was used to activate HIF2α signaling, prevented pulmonary edema and significantly improved mortality in experimental models of sepsis-induced ARDS. Since the same PHD inhibitor is being used in early clinical trials to treat anemia in patients with chronic kidney disease (49), this may also be a feasible and novel approach to treat ARDS patients.

Methods

Reagents. Anti–VE-cadherin (sc-9989, sc-6458, and sc-52751), anti–VE-PTP (SC-28905), anti-HIF2α (sc-13596), anti-PHD2 (sc-271835), anti-sFLT (sc-9029), and anti–β-actin (sc-1616) antibodies were purchased from Santa Cruz Biotechnology Inc.; mouse monoclonal anti–VE-PTP (610180) and anti-HIF1α (610959) antibodies were from BD; anti-HIF3α (ab10134) antibody was purchased from Abcam; anti-HIF2α (NB100-122) antibody was from Novus Biologicals; Lipofectamine 2000, ViraPower Lentiviral Expression System, and Alexa Fluor 488–, 594–, and 633–conjugated secondary antibodies and Alexa Fluor 555–albumin were obtained from Invitrogen; anti–VE-cadherin pY658, pY695, and pY731 antibodies, anti-phosphotyrosine antibody (4G10), and the ChIP assay kit were from EMD Millipore; the luciferase assay kit was purchased from Promega; and the Luminescent β-galactosidase Detection Kit was from Clontech.

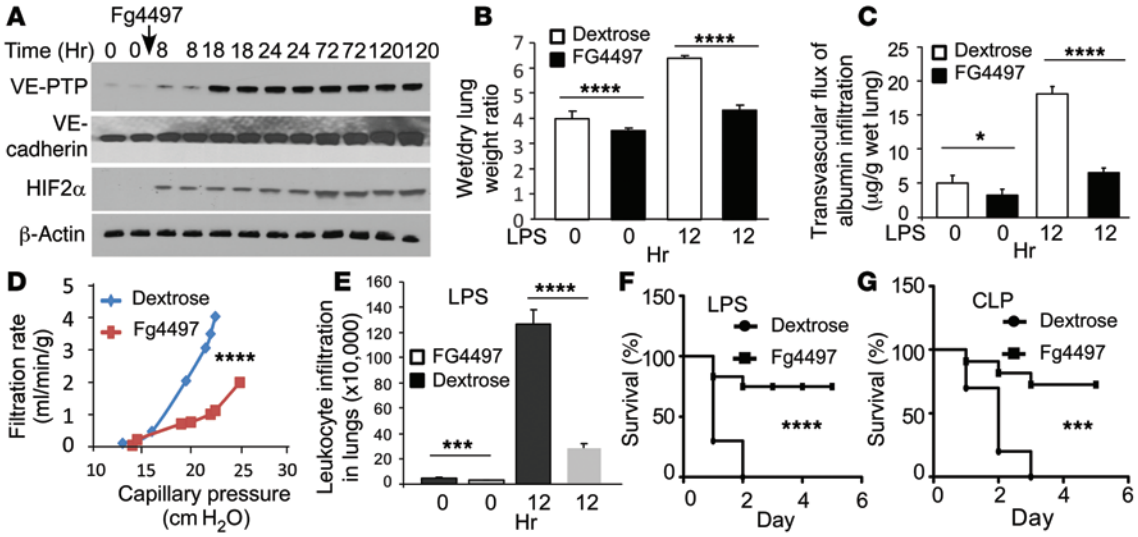

Figure 8. PHD2 inhibition improves lung fluid balance and mortality. (**A**) C57/BL6 mice were challenged with 5% dextrose or 25 mg/kg Fg4497 (same dose thereafter). WB was used to determine expression of the indicated proteins in lungs. (**B** and **C**) Three days after receiving Fg4497, C57/BL6 mice were challenged with PBS or 15 mg/kg LPS. Wet-to-dry lung weight ratios (**B**) and pulmonary transvascular albumin permeability (**C**) were measured. n = 5/group. (**D**) C57/BL6 mice received dextrose or Fg4497, and pulmonary transvascular fluid filtration was measured 3 days later. (**E**) Quantification of leukocytes in BAL fluid from Fg4497-treated mice 12 hours after 15 mg/kg LPS challenge. n = 4/group. $^{****}P < 0.001$ by Student's t test (**B**–**E**). (**F** and **G**) C57/BL6 mice were challenged with 25 mg/kg LPS (**F**) or subjected to CLP (**G**), and then 2 hours later received Fg4497. Survival rates were assessed by log-rank test. $^{***}P < 0.005$; $^{****}P < 0.001$. n = 10/group. Blot images were derived from samples run on parallel gels.

Generation of EC-specific Hif2a$^{-/-}$ mice. For in vivo experiments, we used EC-specific inducible *Hif2a$^{-/-}$* mice generated by i.p. administration of tamoxifen (2 mg/day for 5 days) to *Tie2-Cre Hif2a$^{fl/fl}$* mice (129/B6 background), in which tamoxifen induced expression of a fusion protein of Cre recombinase with the modified estrogen receptor–binding domain (*CreER^{T2}*) under the control of the *Tie2* promoter (50, 51). *Hif2a$^{fl/fl}$* mice were provided by M. Celeste Simon of the University of Pennsylvania (Philadelphia, Pennsylvania, USA) and backcrossed with *Tie2-Cre* recombinase transgenic mice.

Plasmid constructs. Full-length human *Hif1a* and *Hif2a* cDNA plasmids were purchased from Addgene and subcloned into a pLVX-IRES-mCherry vector (Clontech). HIF1α and HIF2α-DPA mutants were generated by overlapping PCR and inserted into the same vector. The plasmid coding for C-terminal mouse VE-PTP from amino acids 1422–1998 was a gift of D. Vestweber (Max Planck Institute for Molecular Biomedicine, Münster, Germany) and subcloned into a pLVX-IRES-mcherry lentiviral vector with a MYC tag. The full-length human *VEPTP* promoter and truncation mutants were PCR amplified from human genomic DNA and inserted into a pGL3-basic vector (Promega). The small double-stranded hairpin siRNAs for HIF1α, HIF2α, HIF3α, and PHDs were designed by BLOCK-iT RNAi Designer (Invitrogen), synthesized by Integrated DNA Technologies (IDT), and inserted into a pLL3.7 lentiviral vector.

Immunofluorescence and confocal microscopy. HLMVECs cultured on coverslips were fixed with 4% paraformaldehyde and permeabilized with 0.1% Triton X-100. Slides were probed with primary antibodies and fluorescence-conjugated secondary antibodies. Images were taken with a Zeiss confocal microscope and analyzed by LSM510 and ImageJ software (NIH).

VE-cadherin cell-surface labeling and endocytosis assays. To visualize the cell surface and internalized VE-cadherin, living ECs were incubated with a BV9 anti–VE-cadherin extracellular domain antibody in the presence of 100 μM chloroquine at 37°C for 4 hours (22). To remove cell-surface–bound antibody, BV9-labeled ECs were subjected to mild acid buffer (2 mM PBS-glycine, pH 2.0, for 2 minutes), washed twice by PBS for 15 minutes (21, 52), and detected with a Zeiss confocal microscope using MLS510 META software.

Co-IP assay. The Co-IP assay was performed as previously reported (53). Cell lysates from HLMVECs exposed to 1% O_2 or Fg4497 were incubated with either a mouse anti–tyrosine phosphorylation antibody, an anti–VE-cadherin antibody, or an equal amount of normal mouse or goat IgG, and then subsequently with protein A– or protein G–conjugated Sepharose beads, followed by Western blot (WB) analysis.

ChIP assay. ChIP was performed using the ChIP Assay Kit (EMD Millipore) according to the manufacturer's protocol. Briefly, HLMVECs cultured in normoxic or 1% O_2 hypoxic conditions were cross-linked by using 1% formaldehyde, washed 3 times with cold PBS supplemented with 1 mM PMSF, and resuspended in cell lysis buffer. The nuclei portion was resuspended in nuclear lysis buffer and sonicated to break down the genomic DNA. After centrifugation, the supernatant was immunoprecipitated with 5 μg anti-HIF1α, HIF2α, or an equal amount of mouse IgG. The DNA obtained from the IP was amplified by PCR with primers specifically recognizing *VEPTP* and VE-cadherin promoters.

Luciferase reporter assays. 293T cells were seeded in 12-well cell culture plates and transfected with the indicated plasmids using Lipofectamine 2000. Two days after transfection, cells were washed in PBS and lysed in reporter lysis buffer. Luciferase and β-gal activity was measured with a Lumat luminometer (Berthold Technologies).

Transendothelial electrical resistance measurements to assess AJ assembly. Confluent HLMVECs plated on gold microelectrodes were

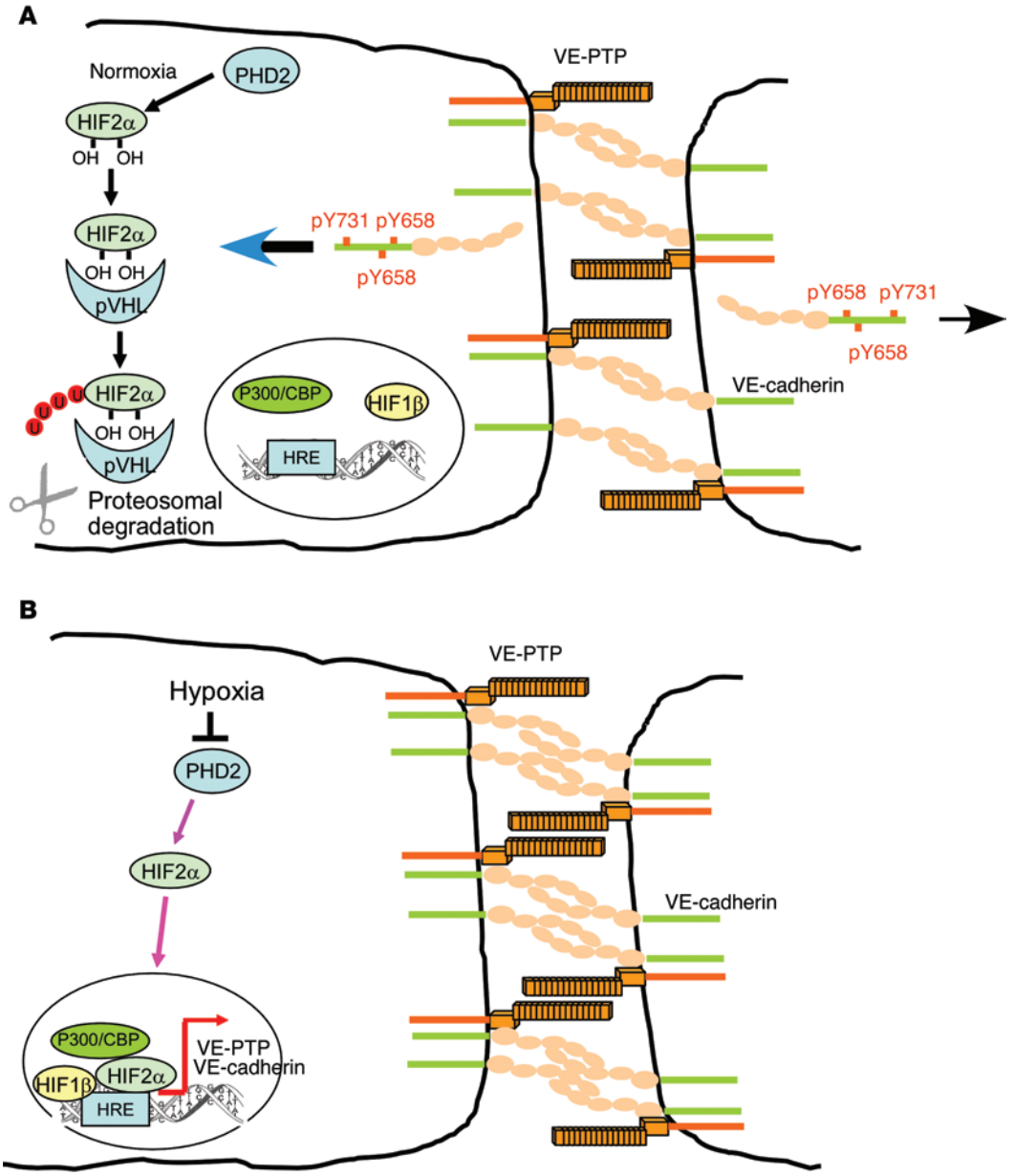

Figure 9. Signaling pathways regulating HIF2α-induced VE-PTP expression. (**A**) In normoxia, PHD2 hydroxylates HIF2α, resulting in its binding to pVHL, which targets HIF2α for proteasomal degradation. Basal levels of VE-PTP and VE-cadherin are expressed in ECs to maintain a restrictive endothelial barrier. VE-PTP–induced dephosphorylation of VE-cadherin maintains VE-cadherin at AJs and prevents VE-cadherin internalization. (**B**) In hypoxia, PHD2 activity is inhibited, and nonhydroxylated HIF2α accumulates in the nucleus and associates with constitutively expressed HIF1β and the coactivator CBP/P300 to transactivate *VEPTP* gene transcription through binding to HREs. VE-PTP interaction with VE-cadherin dephosphorylates VE-cadherin at Y658, Y685, and Y731 and inhibits VE-cadherin internalization, thus enhancing AJ assembly and endothelial barrier integrity.

serum starved and subjected to transendothelial electrical resistance (TER) with LPS challenge. The TER value was monitored with the ECIS system (Applied Biophysics) as previously described (21).

Evans blue–albumin pulmonary transvascular flux measurements. C57/BL6 mice were pretreated with 25 mg/kg Fg4497 or an equal volume of 5% dextrose (vehicle control) by retro-obital injection 3 days before experiments. *Hif2a*$^{fl/fl}$ and *Hif2a*$^{EC-/-}$ mice were prepared with 2 mg tamoxifen i.p. for 5 days as mentioned above. LPS (15 mg/ml) or an equal volume of PBS was given by i.p. injection. Evans blue–albumin (EBA) (40 mg/kg) was injected into the right jugular vein of anesthetized mice and allowed to circulate in the blood vessels for 30 minutes. Intravascular Evans blue was washed by PBS perfusion from the right ventricle for 5 minutes. Mouse lungs were excised, weighed, homogenized in 1 ml PBS, and extracted in 2 ml formamide for 24 hours at 60°C. Evans blue content was determined by OD620 and OD740 of the formamide extract.

Microvessel Kf,c measurements to determine alterations in permeability to liquid. Isolated mouse lungs were perfused in situ from the pulmonary artery with a peristaltic pump, excised, and placed on a force displacement transducer. The lung weight was electronically nulled, and the outflow pressure was then elevated gradually as indicated for 30 minutes. The weight gain was recorded, and the K*f,c* (ml/min/cm H_2O) was calculated from the slope of the weight gain and normalized to the dry lung weight (lungs were dried overnight at 60°C) (54).

Statistics. WB bands were scanned and analyzed for optical density using ImageJ software. Quantification of replicate experiments is presented as the mean ± SD. The log-rank test and a 2-tailed Student's *t* test were used to determine statistical significance, with a *P* value threshold of less than 0.05. Significance levels are indicated in the figures as $^{*}P < 0.05$, $^{**}P < 0.01$, $^{***}P < 0.005$, and $^{****}P < 0.001$.

Study approval. All animal experiments were conducted in accordance with NIH guidelines for the care and use of live animals and

were approved by the IACUC of the University of Illinois.

Acknowledgments

We thank FibroGen Inc. for providing the PHD2-specific inhibitor Fg4497. We thank D. Vestweber for the mouse VE-PTP plasmid. We also thank N. Chen (Department of Pharmacology, University of Illinois) for the luciferase reporter assay and M. Bonini (Department of Pharmacology, University of Illinois) for providing the HIF2α shRNA lentivirus. *Hif2a*$^{fl/fl}$ mice were provided by M. Celeste Simon.

The studies were supported by NIH grants P01 HL60678, R01 HL45638, R01HL118068, and R01 GM094220, and by AHA grant 13SDG16910050.

Address correspondence to: Asrar B. Malik or Jalees Rehman, University of Illinois at Chicago, Department of Pharmacology, 835 South Wolcott Ave., Chicago, Illinois 60612, USA. Phone: 312.996.7635; E-mail: abmalik@uic.edu (A.B. Malik). Phone: 312.996.5552; E-mail: jalees@uic.edu (J. Rehman).

1. Mehta D, Malik AB. Signaling mechanisms regulating endothelial permeability. *Physiol Rev*. 2006;86(1):279–367.
2. Kuppers V, Vockel M, Nottebaum AF, Vestweber D. Phosphatases and kinases as regulators of the endothelial barrier function. *Cell Tissue Res*. 2014;355(3):577–586.
3. Semenza GL. Targeting HIF-1 for cancer therapy. *Nat Rev Cancer*. 2003;3(10):721–732.
4. Farahani RM, Sarrafpour B, Simonian M, Li Q, Hunter N. Directed glia-assisted angiogenesis in a mature neurosensory structure: pericytes mediate an adaptive response in human dental pulp that maintains blood-barrier function. *J Comp Neurol*. 2012;520(17):3803–3826.
5. Appelhoff RJ, et al. Differential function of the prolyl hydroxylases PHD1, PHD2, and PHD3 in the regulation of hypoxia-inducible factor. *J Biol Chem*. 2004;279(37):38458–38465.
6. Kaelin WG, Jr. and Ratcliffe PJ. Oxygen sensing by metazoans: the central role of the HIF hydroxylase pathway. *Mol Cell*. 2008;30(4):393–402.
7. Semenza GL. Regulation of vascularization by hypoxia-inducible factor 1. *Ann N Y Acad Sci*. 2009;1177:2–8.
8. Ivan M, et al. HIFalpha targeted for VHL-mediated destruction by proline hydroxylation: implications for O2 sensing. *Science*. 2001;292(5516):464–468.
9. Epstein AC, et al. C. elegans EGL-9 and mammalian homologs define a family of dioxygenases that regulate HIF by prolyl hydroxylation. *Cell*. 2001;107(1):43–54.
10. Bruick RK, McKnight SL. A conserved family of prolyl-4-hydroxylases that modify HIF. *Science*. 2001;294(5545):1337–1340.
11. Hirsila M, Koivunen P, Gunzler V, Kivirikko KI, Myllyharju J. Characterization of the human prolyl 4-hydroxylases that modify the hypoxia-inducible factor. *J Biol Chem*. 2003;278(33):30772–30780.
12. Mahon PC, Hirota K, Semenza GL. FIH-1: a novel protein that interacts with HIF-1alpha and VHL to mediate repression of HIF-1 transcriptional activity. *Genes Dev*. 2001;15(20):2675–2686.
13. Linke S, Stojkoski C, Kewley RJ, Booker GW, Whitelaw ML, Peet DJ. Substrate requirements of the oxygen-sensing asparaginyl hydroxylase factor-inhibiting hypoxia-inducible factor. *J Biol Chem*. 2004;279(14):14391–14397.
14. Iyer NV, et al. Cellular and developmental control of O2 homeostasis by hypoxia-inducible factor 1 alpha. *Genes Dev*. 1998;12(2):149–162.
15. Tang N, et al. Loss of HIF-1alpha in endothelial cells disrupts a hypoxia-driven VEGF autocrine loop necessary for tumorigenesis. *Cancer Cell*. 2004;6(5):485–495.
16. Tian H, Hammer RE, Matsumoto AM, Russell DW, McKnight SL. The hypoxia-responsive transcription factor EPAS1 is essential for catecholamine homeostasis and protection against heart failure during embryonic development. *Genes Dev*. 1998;12(21):3320–3324.
17. Compernolle V, et al. Loss of HIF-2alpha and inhibition of VEGF impair fetal lung maturation, whereas treatment with VEGF prevents fatal respiratory distress in premature mice. *Nat Med*. 2002;8(7):702–710.
18. Scortegagna M, et al. Multiple organ pathology, metabolic abnormalities and impaired homeostasis of reactive oxygen species in Epas1$^{-/-}$ mice. *Nat Genet*. 2003;35(4):331–340.
19. Skuli N, et al. Endothelial deletion of hypoxia-inducible factor-2alpha (HIF-2α) alters vascular function and tumor angiogenesis. *Blood*. 2009;114(2):469–477.
20. Le Bras A, et al. HIF-2α specifically activates the VE-cadherin promoter independently of hypoxia and in synergy with Ets-1 through two essential ETS-binding sites. *Oncogene*. 2007;26(53):7480–7489.
21. Gong H, et al. Evidence of a common mechanism of disassembly of adherens junctions through Gα13 targeting of VE-cadherin. *J Exp Med*. 2014;211(3):579–591.
22. Xiao K, et al. Cellular levels of p120 catenin function as a set point for cadherin expression levels in microvascular endothelial cells. *J Cell Biol*. 2003;163(3):535–545.
23. Gavard J, Gutkind JS. VEGF controls endothelial-cell permeability by promoting the β-arrestin-dependent endocytosis of VE-cadherin. *Nat Cell Biol*. 2006;8(11):1223–1234.
24. Nottebaum AF, et al. VE-PTP maintains the endothelial barrier via plakoglobin and becomes dissociated from VE-cadherin by leukocytes and by VEGF. *J Exp Med*. 2008;205(12):2929–2945.
25. Yacyshyn OK, Lai PF, Forse K, Teichert-Kuliszewska K, Jurasz P, Stewart DJ. Tyrosine phosphatase beta regulates angiopoietin-Tie2 signaling in human endothelial cells. *Angiogenesis*. 2009;12(1):25–33.
26. Vestweber D, Wessel F, Nottebaum AF. Similarities and differences in the regulation of leukocyte extravasation and vascular permeability. *Semin Immunopathol*. 2014;36(2):177–192.
27. Wessel F, et al. Leukocyte extravasation and vascular permeability are each controlled in vivo by different tyrosine residues of VE-cadherin. *Nat Immunol*. 2014;15(3):223–230.
28. Kim WY, et al. Failure to prolyl hydroxylate hypoxia-inducible factor α phenocopies VHL inactivation in vivo. *EMBO J*. 2006;25(19):4650–4662.
29. Robinson A, Keely S, Karhausen J, Gerich ME, Furuta GT, Colgan SP. Mucosal protection by hypoxia-inducible factor prolyl hydroxylase inhibition. *Gastroenterology*. 2008;134(1):145–155.
30. Shen J, et al. Targeting VE-PTP activates TIE2 stabilizes the ocular vasculature. *J Clin Invest*. 2014;124(10):4564–4576.
31. Komarova YA, Mehta D, Malik AB. Dual regulation of endothelial junctional permeability. *Sci STKE*. 2007;2007(412):re8.
32. He K, et al. Lipopolysaccharide-induced cross-tolerance against renal ischemia-reperfusion injury is mediated by hypoxia-inducible factor-2α-regulated nitric oxide production. *Kidney Int*. 2014;85(2):276–288.
33. Orsenigo F, et al. Phosphorylation of VE-cadherin is modulated by haemodynamic forces and contributes to the regulation of vascular permeability in vivo. *Nat Commun*. 2012;3(1208):1–15.
34. Kapitsinou PP, et al. Endothelial HIF-2 mediates protection recovery from ischemic kidney injury. *J Clin Invest*. 2014;124(6):2396–2409.
35. Goel S, et al. Effects of vascular-endothelial protein tyrosine phosphatase inhibition on breast cancer vasculature and metastatic progression. *J Natl Cancer Inst*. 2013;105(16):1188–1201.
36. Winderlich M, et al. VE-PTP controls blood vessel development by balancing Tie-2 activity. *J Cell Biol*. 2009;185(4):657–671.
37. Ziegler T, et al. Angiopoietin 2 mediates microvascular hemodynamic alterations in sepsis. *J Clin Invest*. 2013;123(8): 3436–3445.
38. Hayashi M, et al. VE-PTP regulates VEGFR2 activity in stalk cells to establish endothelial cell polarity and lumen formation. *Nat Commun*. 2013;4:1672.
39. Vockel M, Vestweber D. How T cells trigger the dissociation of the endothelial receptor phosphatase VE-PTP from VE-cadherin. *Blood*. 2013;122(14):2512–2522.
40. Yuan G, et al. Mutual antagonism between hypoxia-inducible factors 1alpha and 2alpha regulates oxygen sensing and cardio-respiratory homeostasis. *Proc Natl Acad Sci U S A*. 2013;110(19):E1788–E1796.
41. Ogawa S, Gerlach H, Esposito C, Pasagian-Macaulay A, Brett J, Stern D. Hypoxia modulates the barrier and coagulant function of cultured bovine endothelium. Increased monolayer permeability and induction of procoagulant properties. *J Clin Invest*. 1990;85(4):1090–1098.

42. Bland RD, Demling RH, Selinger SL, Staub NC. Effects of alveolar hypoxia on lung fluid and protein transport in unanesthetized sheep. *Circ Res*. 1977;40(3):269–274.
43. Bressack MA, Bland RD. Alveolar hypoxia increases lung fluid filtration in unanesthetized newborn lambs. *Circ Res*. 1980;46(1):111–116.
44. Matthay MA, Ware LB, Zimmerman GA. The acute respiratory distress syndrome. *J Clin Invest*. 2012;122(8):2731–2740.
45. Pipeling MR, Fan E. Therapies for refractory hypoxemia in acute respiratory distress syndrome. *JAMA*. 2010;304(22):2521–2527.
46. Blouin CC, Page EL, Soucy GM, Richard DE. Hypoxic gene activation by lipopolysaccharide in macrophages: implication of hypoxia-inducible factor 1alpha. *Blood*. 2004;103(3):1124–1130.
47. Guzy RD, et al. Mitochondrial complex III is required for hypoxia-induced ROS production and cellular oxygen sensing. *Cell Metab*. 2005;1(6):401–408.
48. Sena LA, Chandel NS. Physiological roles of mitochondrial reactive oxygen species. *Mol Cell*. 2012;48(2):158–167.
49. Bernhardt WM, et al. Inhibition of prolyl hydroxylases increases erythropoietin production in ESRD. *J Am Soc Nephrol*. 2010;21(12):2151–2156.
50. Indra AK, et al. Temporally-controlled site-specific mutagenesis in the basal layer of the epidermis: comparison of the recombinase activity of the tamoxifen-inducible Cre-ER(T) and Cre-ER(T2) recombinases. *Nucleic Acids Res*. 1999;27(22):4324–4327.
51. Korhonen H, et al. Anaphylactic shock depends on endothelial Gq/G11. *J Exp Med*. 2009;206(2):411–420.
52. Gavard J, Patel V, Gutkind JS. Angiopoietin-1 prevents VEGF-induced endothelial permeability by sequestering Src through mDia. *Dev Cell*. 2008;14(1):25–36.
53. Gong H, et al. G protein subunit Galpha13 binds to integrin alphaIIbbeta3 and mediates integrin "outside-in" signaling. *Science*. 2010;327(5963):340–343.
54. Vogel SM, et al. Abrogation of thrombin-induced increase in pulmonary microvascular permeability in PAR-1 knockout mice. *Physiol Genomics*. 2000;4(2):137–145.